Multicentric representation of piecewise constant holomorphic functions and Hermite interpolation

Olavi Nevanlinna, Tiina Vesanen

10.11.2025

Aalto University
Department of Mathematics and Systems Analysis
email: Olavi.Nevanlinna@aalto.fi
Tiina.Vesanen@aalto.fi

Abstract

In multicentric representation of piecewise holomorphic functions one combines Lagrange interpolation at roots of a polynomial p with convergent power series of p as the "coefficients" multiplying the Lagrange basis polynomials. When these power series are truncated one obtains Hermite interpolation polynomials. In this paper we first review different approaches to obtain multicentric representations with emphasis in piecewise constant holomorphic functions.

When the polynomial is of degree d and all power series are truncated after n^{th} power, we formally arrive into a Hermite interpolation polynomial of degree $d(n+1)-1$. The natural way to represent Hermite interpolation is to have for each interpolation condition a basis polynomial which in this case leads to $d(n+1)$ basis polynomials. We then consider the numerical accumulation of errors in the different ways to represent and evaluate the Hermite interpolation. In the multicentric representation due to the convergence of the power series, numerical errors stay bounded as n grows. When we assume that the piecewise constant holomorphic function takes the value 1 in one of the components and vanishes in the other so that the Hermite interpolation agrees with just one basis polynomial, even then the truncated multicentric representation is favorable. In the general case one would take a linear combination of all $d(n+1)$ basis polynomials.

Keywords: multicentric calculus, polynomial as new variable, piecewise constant functions , Hermite interpolation, holomorphic functional calculus, Riesz projections

MSC (2020): 47-02, 47A55, 47A60, 47B99

1 Introduction

Using *multicentric calculus* [10] it is possible to get stable and convergent power series based representations for piecewise constant holomorphic functions. When these series expansions are truncated, we obtain polynomials which formally agree with polynomials obtained as Hermite interpolants. In this paper we present different ways of creating the multicentric representations. Then we comment different ways of creating Hermite interpolants for the same purpose. All these different representations can be done with exact arithmetics, but we shall then compare their performance under assumptions where we allow in evaluations of variables tiny errors. In the representations obtained from the multicentric form the errors do not accumulate essentially at all, unlike in the other expressions.

While with Hermite interpolation we may form a basis from polynomials, of which the interpolative polynomial can be obtained as linear combination, in multicentric representation we use a fixed Lagrangian interpolation basis but consider the coefficients as functions. And it is the series expansions of these "coefficients" which when truncated yield formally the Hermite interpolant. This is the cause for a very different order of steps in evaluating the polynomials and is visible in the sensitivity in error propagation.

Different approaches to get the multicentric representations are surveyed in Section 2 but the point of departure is in *taking a polynomial as a new variable*. We assume that a polynomial p of degree d with simple roots λ_k has been selected and the lemniscate set

$$V(\rho) = \{z \in \mathbb{C} : \ |p(z)| \leq \rho\}$$

has several components. In *multicentric calculus* we represent scalar functions

$$\varphi : V(\rho) \to \mathbb{C}, \ \ z \mapsto \varphi(z)$$

by vector valued functions

$$f : B(\rho) \to \mathbb{C}^d, \ \ w \mapsto f(w)$$

so that if $z \in V(\rho)$ then the new variable $w = p(z)$ is in the disc $B(\rho)$ and within the lemniscate

$$\gamma_\rho = \{z \in \mathbb{C} : \ |p(z)| = \rho\}.$$

The original function can then be recovered by

$$\varphi(z) = \sum_{k=1}^{d} \delta_k(z) f_k(p(z)) \tag{1.1}$$

where the polynomial δ_k is, as in the Lagrange interpolation, the polynomial of degree $d-1$ such that $\delta_k(\lambda_k) = 1$, while $\delta_k(\lambda_j) = 0$ for $j \neq k$.

Jacobi [5] considered (without the Cauchy integral) expansions of the form

$$\varphi(z) \sim \sum_{j=0}^{\infty} c_j(z) p(z)^j$$

where c_j are polynomials of degree less than d, see e.g. [7, 4, 13, 8]. However, in this tradition $w = p(z)$ was not considered a truly new variable. Hence, the real potential of utilising power series in discs for computational purposes was overlooked. We call this multicentric calculus; observe that $|p(z)|^{1/d}$ is the geometric average of distances from z to the "local centers" λ_k. On this development see [10, 9, 3, 11, 1], but we aim here to be sufficiently self-contained.

An important application of multicentric calculus is in holomorphic functional calculus, where one needs an accurate and and easily computable approximation of holomorphic functions φ near the spectrum $\sigma(A)$ of a given bounded operator A. When the spectrum lies inside the components bounded by the lemniscate, then the spectrum of $B = p(A)$ lies inside the corresponding disc and if we have power series

$$f_k(w) = \sum_{j=0}^{\infty} \alpha_{k,j} w^j$$

available and converging fast, then only a moderate number of terms of the power series is needed to represent $f_k(B)$, after which an approximation of

$$\varphi(A) = \sum_{k=1}^{d} \delta_k(A) f_k(B)$$

can be computed. Notice that if, say for a sparse large scale matrix A, the matrix $\varphi(A)$ is only needed at a vector b, then all multiplications needed to create the approximate $\varphi(A)b$ can be obtained using matrix-vector multiplications only.

Here we concentrate on holomorphic functions which are piecewise constant. However, this can be done by further narrowing the focus on *functions which are identically* 1 *in one component and vanish in the others* as the general case can be obtained by superposing. In this approach we have approximation errors mainly from the truncation of power series of the components of f and numerical errors from evaluation of the truncated expansions at the operator or matrix $B = p(A)$. However, it is important to notice that we have the liberty to choose the local centers λ_k to have rational real and imaginary parts as then in the multicentric representation the coefficients in the power series of the components of f are all rational, and the computations to create them can be done with exact arithmetic.

Proposition 1.1. *Assume that all roots λ_k of p have rational real and imaginary parts. If φ is holomorphic at the roots and all values $\varphi^{(\nu)}(\lambda_k)$ have also rational real and imaginary parts then the series expansions of f_k have coefficients with rational real and imaginary parts only.*

Proof. This follows immediately from the explicit recursion, see [10, 1] or (2.11) below. □

We use the following notation for truncating power series. If

$$a(x) \sim \sum_{j=0}^{\infty} c_j x^j, \quad \text{then } \lfloor a \rfloor_n(x) = \sum_{j=0}^{n} c_j x^j. \tag{1.2}$$

Thus, when we truncate the series for $f_k(w)$ we can write at $w = p(z)$

$$\lfloor f_k \rfloor_n(p(z)) = \sum_{j=0}^{n} \alpha_{k,j}\, p(z)^j. \tag{1.3}$$

Consider now the Hermite interpolation problem: at d distinct complex points λ_k to find polynomial P such that

$$P^{(\nu)}(\lambda_k) = a_{k,\nu} \text{ for } \nu = 0, \ldots, n; \quad k = 1, \ldots, d. \tag{1.4}$$

Proposition 1.2. *Let φ be holomorphic at interpolation points λ_k. Then the truncated polynomial of the multicentric representation of φ*

$$P(z) = \sum_{k=1}^{d} \delta_k(z) \lfloor f_k \rfloor_n (p(z))$$

is the unique polynomial of degree $N \leq d(n+1) - 1$ satisfying the interpolation problem (1.4) when $a_{k,\nu} = \varphi^{(\nu)}(\lambda_k)$.

Proof. Clearly, P is of at most degree $d(n+1) - 1$. Consider the difference $\varphi - P$. We have

$$\varphi(z) - P(z) = p(z)^{n+1} \sum_{k=1}^{d} \delta_k(z) \sum_{j=n+1}^{\infty} \alpha_{k,j}\, p(z)^{j-n-1}$$

which shows that the interpolation conditions are all satisfied. □

Denote by $\delta_{k,j,n}$ the solution to the special case of (1.4) with $a_{k,j} = 1$, while $a_{m,\nu} = 0$ when $(m, \nu) \neq (k, j)$. Then $(\delta_{k,j,n})$ is a basis such that the general problem (1.4) is solved by

$$P(z) = \sum_{k=1}^{d} \sum_{j=0}^{n} a_{k,j}\ \delta_{k,j,n}(z).$$

We shall keep writing φ and f when we discuss general formulae but use χ and g in the particular case where $\chi(z) = 1$ in the component containing the root λ_1 and vanishing in the components containing other roots, so that

$$\chi(z) = \sum_{k=1}^{d} \delta_k(z) g_k(p(z)).$$

When we truncate here the power series of g_k's we get the basis function $\delta_{1,0,n}$ which has the multicentric representation

$$\delta_{1,0,n}(z) = \sum_{k=1}^{d} \delta_k(z) \lfloor g_k \rfloor_n (p(z)). \tag{1.5}$$

This representation of the polynomial $\delta_{1,0,n}$ is later denoted by M_n, letter M for multicentric.

In Section 3 we indicate different direct ways to evaluate this basis polynomial. With H_n we denote the direct representation as powers of z, S_n shall denote a special representation of the basis polynomial and T_n is reserved for a particular formulation of the basis polynomial suitable for parallel computing.

In Section 4 we consider the numerical stability of these different ways and in particular see that the order of computational steps obtained from truncation the multicentric representation is superior, as we let n grow while keeping the interpolation points, the roots of p fixed. More specifically, we shall demonstrate their different sensitivity using the following two polynomials, one with real zeros symmetrically around he origin

$$p(z) = z(1 - z^2) \tag{1.6}$$

and another, nonsymmetric one:

$$p(z) = z(z^2 + 4z + 5). \tag{1.7}$$

In both polynomials we choose $\lambda_1 = 0$ to be the root lying in the component where the piecewise holomorphic function would be identically 1. Thus, the first one models a situation where we would be using Riesz functional calculus to concentrate in the middle of the spectrum while the second could be thought as modelling a situation where one would like to identify the invariant subspace of an operator corresponding to the unstable part of the spectrum. Notice that the behaviors are independent of translating and scaling of the basic variable z.

2 Basic formulas for multicentric representation

In this section we present different approaches to create the multicentric representations for holomorphic functions. Formulas are given for general holomorphic functions φ, and then f is used for the vector valued representing function, while for piecewise constant functions we use χ with g as the representing function, as the formulas simplify considerable. We begin with splitting the Cauchy kernel and then obtain the general integral representations for the components of f. The integral representation can be used to obtain effective bounds for the truncation errors and for the speed of the convergence. Then we remind that the contour integrals can be obtained by residue calculus. A completely different starting point is to use the polyproduct algebra for which the functional equation $\chi^2 = \chi$ allows one to make a power series ansatz for g and to solve the coefficients recursively from $g \circledcirc g = g$. Finally, if we are given φ as a power series of the original variable z, then we can obtain f from knowing $Z_j^{\circledcirc k}$ which represents z^k by transforming the power series termwise.

2.1 Cauchy integrals

Assume ρ is such that the lemniscate γ_ρ does not pass through any critical point of p. We decompose the Cauchy kernel in order to get integral representation for the components of the vector function $f(w)$, see [10].

We decompose the Cauchy kernel $\frac{1}{\lambda - z}$ writing

$$\frac{1}{\lambda - z} = \frac{1}{p(\lambda) - p(z)} \sum_{k=1}^{d} p'(\lambda_k)\delta_k(\lambda)\delta_k(z). \tag{2.1}$$

Denoting

$$K_k(\lambda, w) = \frac{1}{\lambda - \lambda_k} \frac{p(\lambda)}{p(\lambda) - w} \tag{2.2}$$

we obtain for f_k the expression

$$f_k(w) = \frac{1}{2\pi i} \int_{\gamma_\rho} K_k(\lambda, w)\varphi(\lambda) d\lambda, \tag{2.3}$$

where φ is holomorphic inside γ_ρ and continuous up to boundary. Here we are interested in piecewise continuous φ which means that if the lemniscate would pass through a critical point, then φ would have to take the same value in each component touching this critical point. Without loss on generality we assume that ρ is such that the lemniscate contains no critical points and in particular the lemniscate consists of smooth curves, each surrounding at least one λ_k. Then, if $|w| < |p(\lambda)| = \rho$, the series

$$f_k(w) = \sum_{n=0}^{\infty} \alpha_{k,n} w^n$$

converges where

$$\alpha_{k,n} \;=\; \frac{1}{2\pi i} \int_{\gamma_\rho} \frac{1}{\lambda - \lambda_k} \, \frac{\varphi(\lambda)}{p(\lambda)^n} \, d\lambda. \tag{2.4}$$

We shall assume that χ takes only values 1 and 0, as by linearity the other piece wise constant functions can be expressed as linear combination of those.

Example 2.1. Let $p(z) = z(1 - z^2)$ and set $\lambda_1 = 0, \lambda_2 = -1, \lambda_3 = 1$, so that

$$\delta_1(z) = 1 - z^2, \;\; \delta_2(z) = \frac{1}{2}(z^2 - z) \;\text{ and }\; \delta_3(z) = \frac{1}{2}(z^2 + z). \tag{2.5}$$

Consider the piecewise holomorphic χ which vanishes at ± 1 and takes the value 1 at origin. The critical points are $\pm 1/\sqrt{3}$ and corresponding critical values $\pm 2/3\sqrt{3}$, and hence χ has a multicentric representation with g_j given as a converging power series in $|w| < |2/3\sqrt{3}| = \rho_{crit} \approx 0,385$. Let $r > 0$ be small enough so that along $|z| = r$ we have $|p(z)| < \rho_{crit}$, that is $r(1 + r^2) < \rho_{crit}$, then we have from (2.4)

$$\alpha_{1,n} = \; \frac{1}{2\pi i} \int_{|\lambda| = r} \frac{1}{\lambda^{n+1}} \, \frac{1}{(1 - z^2)^n} \, d\lambda, \tag{2.6}$$

while

$$\alpha_{2,n} = \; \frac{1}{2\pi i} \int_{|\lambda| = r} \frac{1}{\lambda^n} \, \frac{1}{(\lambda + 1)(1 - z^2)^n} \, d\lambda, \tag{2.7}$$

and

$$\alpha_{3,n} = \; \frac{1}{2\pi i} \int_{|\lambda| = r} \frac{1}{\lambda^n} \, \frac{1}{(\lambda - 1)(1 - z^2)^n} \, d\lambda. \tag{2.8}$$

The integrals are obtained easily with residue calculus:

$$\begin{aligned}
g_1(w) &= 1 \quad + 2w^2 \quad + 10w^4 \quad + 56w^6 \quad + 330w^8 + \cdots \\
g_2(w) &= \quad w - w^2 + 4w^3 - 5w^4 + 21w^5 - 28w^6 + 120w^7 - 165w^8 + \cdots \\
g_3(w) &= -w - w^2 - 4w^3 - 5w^4 - 21w^5 - 28w^6 - 120w^7 - 165w^8 - \cdots
\end{aligned}$$

Example 2.2. Let now $p(z) = z(z^2 + 4z + 5)$. Here again we have $\chi(0) = 1$ while χ vanishes at $\lambda_j = -2 \pm i$. Here the critical radius $\rho_{crit} = 2$. The components of g are:

$$\begin{aligned}
g_1(w) &= 1 - \frac{4}{5^2}\, w + \frac{38}{5^4}\, w^2 - \frac{16}{5^4}\, w^3 + \frac{882}{5^7}\, w^4 - \ldots \\
g_2(w) &= + \frac{2+i}{5^2} w - \frac{19+12i}{5^4} w^2 + \frac{40+28i}{5^5} w^3 - \frac{441+328i}{5^7} w^4 + \ldots \\
g_3(w) &= + \frac{2-i}{5^2} w - \frac{19-12i}{5^4} w^2 + \frac{40-28i}{5^5} w^3 - \frac{441-328i}{5^7} w^4 + \ldots
\end{aligned}$$

In our numerical tests these expansions are truncated. As the expansions converge in discs $|w| \le r < \rho_{crit}$, we have uniform bounds for the numerical errors, independent of the degree of the approximation, see Section 2.6.

2.2 Using residue calculus

For the convenience of the reader we give the formulas for the residue calculus. Suppose $\varphi = 1$ inside a component containing λ_j and for simplicity, that ρ is small enough so that all other λ_k's are outside this component. We need to calculate the residues at λ_j of the terms in the power series of

$$K_k(z,w) = \frac{1}{z-\lambda_k} \sum_{n=0}^{\infty} \frac{w^n}{p(z)^n}. \tag{2.9}$$

In general, if $g(z)$ has pole at z_0 of order m so that m is the smallest integer for which $(z-z_0)^m g(z)$ is analytic at z_0 then the *residue* at z_0 is given by the formula

$$res(g, z_0) = \frac{1}{(m-1)!} \lim_{z \to z_0} \frac{d^{m-1}}{dz^{m-1}} [(z-z_0)^m g(z)] \tag{2.10}$$

Now, in the series of $K_j(z,w)$ the function multiplying w^n has a pole at λ_j of order $n+1$. Factor $p(z) = (z-\lambda_j)q_j(z)$. Then the residue is obtained as

$$\alpha_{j,n} = \frac{1}{n!} \lim_{z \to \lambda_j} \frac{d^n}{dz^n} q_j^{-n},$$

and

$$\frac{1}{2\pi i} \int_{\gamma_j} K_j(z,w)dz = \sum_{n=0}^{\infty} \alpha_{j,n} w^n$$

where the series converges for small enough w. In a similar way, with $K_k(z,w)$ the term multiplying w^n has a pole at λ_j of order n. Thus $\alpha_{k,0} = 0$ and for $n \ge 1$

$$\alpha_{k,n} = \frac{1}{(n-1)!} \frac{d^{n-1}}{dz^{n-1}} \left(\frac{1}{(z-\lambda_k)q_j(z)^n} \right).$$

2.3 Recursion by differentiating

If we differentiate the holomorphic φ in (1.1) and assume the data $\varphi^{(\nu)}(\lambda_k)$ to be given, then an explicit recursion for $\alpha_{j,\nu} = f_j^{(\nu)}(0)/\nu!$ is obtained from

$$p'(\lambda_j)^\nu f_j^{(\nu)}(0) = \varphi^{(\nu)}(\lambda_j) - t_{j,\nu}, \tag{2.11}$$

where

$$t_{j,\nu} = \sum_{k=1}^{d} \sum_{\mu=0}^{\nu-1} \binom{\nu}{\mu} \delta_k^{\nu-\mu}(\lambda_j) \sum_{l=0}^{\mu} b_{\mu,l}(\lambda_j) f_k^{(l)}(0) + \sum_{l=0}^{\nu-1} b_{\nu,l}(\lambda_j) f_j^{(l)}(0)$$

and the polynomials $b_{\nu,l}$ are obtained from a triangular table, see [10, 2].

2.4 Solving $g \circledcirc g = g$

In [11] a polyproduct $f \circledcirc g$ was defined such that if f and g represent φ and ψ, then $f \circledcirc g$ represents $\varphi\psi$. Since $\chi^2 = \chi$ we can obtain the expansions for the components of g by subsituting an Ansatz for each of the component, which leads again to an explicit recursion for the coefficients. For $g_k(w) = \sum_{n=1}^{\infty} \alpha_{k,n} w^n$ we get

$$\alpha_{k,n+1}(1-2\alpha_{k,0}) = \sum_{l=1}^{n} \alpha_{k,l}\,\alpha_{k,n+1-l} - \sum_{m \neq k} \sigma_{km} \sum_{l=0}^{n} (\alpha_{k,l}-\alpha_{m,l})(\alpha_{k,n-l}-\alpha_{m,n-l}). \tag{2.12}$$

In the symmetrical case of χ the starting values are $\alpha_{1,0} = 1$ and $\alpha_{2,0} = \alpha_{3,0} = 0$. For the first step ($n = 0$) (2.12) simplifies to

$$\begin{aligned} \alpha_{1,1}\underbrace{(1-2\alpha_{1,0})}_{=-1} &= -\sum_{m\neq 1} \sigma_{1m}(\alpha_{1,l}-\alpha_{m,l})^2 \\ &= \sigma_{1,2} + \sigma_{1,3} = -\frac{1}{2} + \frac{1}{2} = 0, \end{aligned}$$

and for $k = 2$

$$\alpha_{2,1}\underbrace{(1-2\alpha_{2,0})}_{=1} = \sigma_{2,1}\cdot 1^2 + \sigma_{2,3}\cdot 0^2 = -1,$$

i.e. $\alpha_{2,1} = -1$ and similarly for $k = 3$ we get $\alpha_{3,1} = 1$.

2.5 Formulas for z^k

In case one has the plain expression $H_n(z)$ available with exact coefficients, it is desirable to transform it to truncated multicentric form M_n. To that end we list the formulas for transforming the powers z^k. Denote by $Z^{\circledcirc k}$ the vector function representing z^k, so that

$$z^k = \sum_{j=1}^{d} \delta_j(z)\,(Z^{\circledcirc k})_j(p(z)).$$

Using the polyproduct we have from $Z^{\circledcirc (k+1)} = Z \circledcirc Z^{\circledcirc k}$

$$(Z^{\circledcirc (k+1)})_j(w) = \lambda_j (Z^{\circledcirc k})_j(w) + w \sum_{l=1}^{d} \frac{(Z^{\circledcirc k})_l(w)}{p'(\lambda_l)}, \tag{2.13}$$

see [12].

For example in the symmetrical example $p(z) = z(1-z^2)$, the Hermite polynomial with $n = 2$ is $H_2(z) = (1-z^2)^2 = 1 - 2z^2 + z^4$. The multicentric representation for z^2 comes directly from Lagrange interpolation formula,

$$z^2 = \sum_{j=1}^{3} \delta_j(z)\lambda_j^2,$$

and the powers z^3 and z^4 are calculated with the recursion formula as follows,

$$z^3 = \sum_{j=1}^{3} \delta_j(z)\left(\lambda_j^3 + w\sum_{l=1}^{3} \frac{\lambda_l^2}{p'(\lambda_j)}\right) = \sum_{j=1}^{3} \delta_j(z)\left(\lambda_j^3 - w\right)$$

and

$$z^4 = \sum_{j=1}^{3} \delta_j(z) \left(\lambda_j(\lambda_j^3 - w) + w \sum_{l=1}^{3} \frac{\lambda_j^3 - w}{p'(\lambda_j)} \right) = \sum_{j=1}^{3} \delta_j(z) \left(\lambda_j^4 - \lambda_j w \right).$$

Combining the results we have M_2 representing H_2 in the form

$$M_2(z) = \sum_{j=1}^{3} \delta_j(z) \left(1 - 2\lambda_j^2 + \lambda_j^4 - \lambda_j p(z) \right).$$

2.6 Errors due to inexact evaluation of the variables

We can use the integral representation from Section 2.1 to derive bounds for the accumulated errors. Let φ be holomorphic for $|p(z)| < r$ and denote for $\rho < r$

$$M(\rho) = \max_{|p(z)| \le \rho} |\varphi(z)|.$$

We assume here that the exact values of coefficients $\alpha_{k,j}$ can be used, as this is the case e.g. when the roots λ_k have rational real and imaginary parts and φ takes only integer values.

Let us denote

$$D(\rho) = \max_{k} \max_{|p(z)| \le \rho} |\delta_k(z)|,$$

and $L(\rho) = \sum_{k=1}^{d} L_k(\rho)$ where

$$L_k(\rho) = \frac{1}{2\pi} \int_{\gamma_\rho} \frac{|d\lambda|}{|\lambda - \lambda_k|}.$$

Then we have from (2.4)

$$|\alpha_{k,j}| \le \; M(\rho) \, L_k(\rho) \, \rho^{-j}.$$

Consider now bounding f_k for $|w| \le \rho_0$ where $\rho_0 < \rho$. We have immediately

$$\max_{|w| \le \rho_0} |f_k(w)| \le M(\rho) \, L_k(\rho) \, \frac{\rho}{\rho - \rho_0}.$$

As the coefficients $\alpha_{k,j}$ can be computed exactly, we focus on the effect caused by nonexact evaluation of the variables z and $w = p(z)$. We denote by their inexact evaluations by $\hat{z}$ and by $\hat{w}$ and allow the approximations to differ each time when applied.

Let $\rho_0 < \rho_1 < \rho$. We require the approximations to satisfy the following. On the evaluation of basis polynomials we require

$$\max_{|p(z)| \le \rho_0} |\delta_k(\hat{z})| \le \max_{|p(z)| \le \rho_1} |\delta_k(z)| \tag{2.14}$$

$$\max_{|p(z)| \le \rho_0} |\delta_k(z) - \delta_k(\hat{z})| \le \varepsilon_0 \tag{2.15}$$

and on the evaluations of the polynomial variable

$$\max_{|p(z)| \le \rho_0} |\hat{w}| \le \rho_1, \tag{2.16}$$

$$\max_{|p(z)|\le\rho_0} |p(z)-\hat{w}| \le \varepsilon_1. \tag{2.17}$$

Finally, for the approximation of φ at the point z we write

$$\hat{\varphi}(z) = \sum_{k=1}^{d} \delta_k(\hat{z}) f_k(\hat{w}).$$

Then we have the following bound for the total error in $\varphi(z)$ inside the lemniscate $|p(z)| = \rho_0$.

Proposition 2.3. *If $|p(z)| \le \rho_0$, and the assumptions above hold, we have*

$$|\varphi(z) - \hat{\varphi}(z)| \le M(\rho)L(\rho) \{ \frac{\rho}{\rho-\rho_0}\, \varepsilon_0 + D(\rho_1) \frac{\rho_1}{(\rho-\rho_1)^2}\, \varepsilon_1 \}. \tag{2.18}$$

Proof. We have

$$|\varphi(z) - \hat{\varphi}(z)| \le \sum_{k=1}^{d} |\delta_k(z) - \delta_k(\hat{z})|\, |f_k(p(z))| + \sum_{k=1}^{d} |\delta_k(\hat{z})|\, |f_k(p(z)) - f_k(\hat{w})|. \tag{2.19}$$

The first term on the right of (2.19) gives immediately the first term on the right of (2.18). To get the second term write

$$|p(z)^j - \hat{w}^j| \le (j-1)\, \rho_1^{j-1} \varepsilon_1.$$

□

Remark 2.4. If the series expansions are truncated, then the error bound holds for the truncated versions M_n without modifications, or if one wants, the infinite series can be replaced by their, smaller, truncated versions.

3 Formulas for related Hermite interpolation

Denoting by $\delta_{k,j,n}$ the basis polynomials of degree $N = d(n+1) - 1$ satisfying for $k, l = 1, \dots, d$ and $j, m = 0, \dots, n$

$$\delta_{k,j,n}^{(m)}(\lambda_l) = 1 \text{ when } k = l \text{ and } j = m, \text{while vanish otherwise} \tag{3.1}$$

we can write the general Hermite polynomials as linear combinations of these, see (1.4).

We restrict our numerical studies in the particular case of just one basic polynomial, that of $\delta_{1,0,n}$. This basis polynomial has a simple form and we compare the numerical stability of evaluating it as n grows, with the representation obtained from truncating the multicentric representation.

We begin with a simple observation of the form of $\delta_{1,0,n}$, which we denote by S_n. Here, as before δ_1 denotes the Lagrange interpolation polynomial taking value 1 at λ_1.

Proposition 3.1. *We have*

$$S_n = \delta_1^{n+1} \lfloor \delta_1^{-n-1} \rfloor_n. \tag{3.2}$$

Proof. We may assume that $\lambda_1 = 0$. Clearly $\delta_1(z)^{n+1} \lfloor \delta_1^{-n-1} \rfloor_n(z)$ vanishes at least $n+1$ times at every λ_k with $k \geq 2$. On the other hand, for small z we have

$$\delta_1(z)^{n+1} \lfloor \delta_1^{-n-1} \rfloor_n(z) = 1 + \mathcal{O}(z^{n+1})$$

and hence it is the basis polynomial $\delta_{1,0,n}$. □

Remark 3.2. Since $\delta_1(z) = 1 - \sum_{k=2}^{d} \delta_k(z)$ we have

$$\delta_1(z)^{-n-1} = \sum_{m=0}^{\infty} \binom{n+m}{n} Q(z)^m$$

where $Q(z) = \sum_{k=2}^{d} \delta_k(z)$.

Example 3.3. Returning to the special case of $p(z) = z(1-z^2)$ we obtain for example

$$S_3(z) = (1-z^2)^4(1+4z^2) \text{ and } S_4(z) = (1-z^2)^5(1+5z^2+15z^4).$$

In [6] an algorithm to evaluate Hermite polynomials, particularly suitable for parallel computation is given. Modifying it into our test case it reduces to the form

$$T_n = \delta_1^{n+1} \sum_{k=1}^{d} s_{n+1,k} \tag{3.3}$$

where the polynomials $s_{n+1,k}$ are given as follows:

$$s_{n+1,k}(z) = \begin{bmatrix} 1 & \frac{z}{1!} & \dots & \frac{z^n}{n!} \end{bmatrix} \begin{bmatrix} c_{j,1} \\ \vdots \\ c_{j,n+1} \end{bmatrix} = c_{j,1} + \frac{c_{j,2}}{1!} z + \dots + \frac{c_{j,n+1}}{n!} z^n.$$

The vector $[c_{j,m}]$ is obtained as follows.

Kechriniotis et al. derive in [6] (in our notation) that,

$$h_n(z) = \sum_{j=1}^{d} \sum_{k=1}^{n+1} X_{j,n+1}(I_{n+1} - \Lambda_j)^{k-1} A_j,$$

for the general case $h_n^{(j)}(\lambda_i) = a_{ij}$. Here

$$X_{j,n+1} = \delta_j(z)^{n+1} \begin{bmatrix} 1 & \frac{(z-\lambda_j)}{1!} & \dots & \frac{(z-\lambda_j)^n}{n!} \end{bmatrix},$$

and Λ_k is a lower triangular matrix $[l_{k,ij}]$ with

$$l_{k,ij} = \binom{i-1}{j-1} L_{k,n+1}^{(i-j)}(\lambda_k)$$

and $L_{k,n+1}(z) = \delta_k(z)^{n+1}$, and A_j is the j^{th} column of data from $[a_{ij}]$.

For χ this simplifies to

$$T_n(z) = \delta_1^{n+1}(z) \cdot \sum_{k=1}^{d} \underbrace{\begin{bmatrix} 1 & \frac{z}{1!} & \dots & \frac{z^n}{n!} \end{bmatrix} \begin{bmatrix} c_{k,1} \\ \vdots \\ c_{k,n+1} \end{bmatrix}}_{=s_{n+1,k}(z)},$$

where $[c_{j,m}]$ is the first column of matrix $(I_{n+1} - \Lambda_1)^j$.

4 Numerical experiments

We denote by

$$M_n(z) = \sum_{k=1}^{d} \delta_k(z) \lfloor g_k \rfloor_n (p(z)), \tag{4.1}$$

$$S_n(z) = \delta_1(z)^{n+1} \lfloor \delta_1^{-n-1} \rfloor_n (z) \tag{4.2}$$

and

$$T_n(z) = \delta_1(z)^{n+1} \sum_{k=1}^{d} s_{n+1,k}(z) \tag{4.3}$$

the *same* polynomial

$$H_n(z) = \sum_{j=0}^{N} a_j z^j, \tag{4.4}$$

written in different ways, in order to compare the accumulation of different errors. Here all polynomials are of degree $N \leq d(n+1) - 1$ but we list them to be indexed by n, i.e. the number of rounds of derivative data used. Thus p (and hence d) are kept fixed.

Each of the component polynomials, e.g. $p(z)$, $\lfloor \delta_1^{-n-1} \rfloor_n(z)$, etc. and in the case of Hermite polynomial $H_n(z)$, are evaluated using Horner's method. We will add two kinds of errors to the Horner's method.

First we add an *evaluation error* of size ν to the point of evaluation z. It is added once to the test point z. For example instead of $az^2 + bz + c = c + z(b + z \cdot a)$ we use

$$az^2 + bz + c \approx c + \hat{z}(b + \hat{z}a).$$

Here $\hat{z}$ is of form $z + (a + ib)$ where $|a| < \nu$ and $|b| < \nu$.

The second source of error added to the Horner's method is the *rounding error* of size μ after each arithmetic operation. We use the formula

$$b + \hat{z}a \approx (\, b + (\hat{z}a)(1 + \mu_1)\,)\,(1 + \mu_2),$$

for the error, where μ_i:s, $i = 1, 2$, are random complex numbers with real and imaginary parts of size less than μ.

The third source of errors comes from the location of the evaluation point z. As we saw in section 2.6 the error in inexact evaluation can grow larger with the distance from the roots, i.e. the levels ρ of the lemniscate γ_ρ.

The fourth source of errors present with all previous sources is the double precision floating point arithmetics used in the calculations. To minimize other sources of errors we calculate the coefficients of the component polynomials and the exact value $H_n(z)$ algebraically before converting them to floating point numbers.

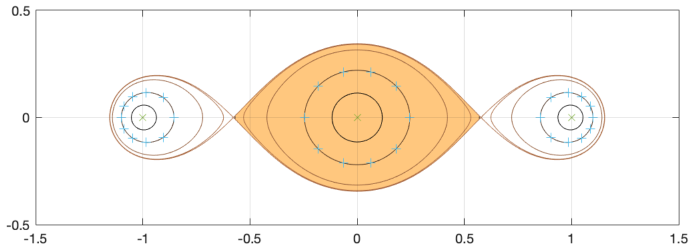

Figure 1: (Example 1) Level curves of polynomial $p(z) = z(1-z^2)$ with roots $\lambda_1 = 0$, $\lambda_2 = -1$, and $\lambda_3 = +1$. The roots are marked with 'x'. The critical points c, from $p'(c) = 0$, are $c = \pm 1/\sqrt{3} \approx \pm 0.577$. At corresponding level $|p(c)| = 2/(3\sqrt{3}) =: \rho_{crit} \approx 0.3849$ the three components join together. The piecewise constant function χ we approximate with Hermite polynomials is 1 at $\lambda_1 = 0$ and 0 at the other two roots. The component enclosing $\lambda_1 = 0$ is colored. Four sets of smaller level curves γ_ρ where ρ is $t \times \rho_{crit}$ and t is either 0.30, 0.60, 0.90 or 0.99 are drawn in addition to the lemniscate $|p(z)| = \rho_{crit}$. Example of the testpoints used in our numerical calculations are marked with '+' on the lemniscate $|p(z)| = 0.6 \times \rho_{crit}$.

ρ	Example 1	Example 2
$0.3 \times \rho_{crit}$	0.1155	0.60
$0.6 \times \rho_{crit}$	0.2309	1.20
$0.9 \times \rho_{crit}$	0.3464	1.80
$0.99 \times \rho_{crit}$	0.3811	1.98

Table 4.1: In Example 1 ρ_{crit} is $2/3\sqrt{3} \approx 0.3849$ and in Example 2 ρ_{crit} is 2. The images of lemniscates γ_ρ are drawn in Figure 1 and 2 respectively.

4.1 Testpoints

We use two previously mention cases in Example 2.1 and Example 2.2 for our numerical examples. For simplicity we use the names Example 1 and Example 2 from now on. Images of the examples are in Figures 1 and 2. In both cases the ρ_{crit} refers to the critical level, i.e. to the lemniscate γ_ρ, where the area with $\chi \equiv 1$ makes a contact with the area(s) where $\chi \equiv 0$.

For each ρ and lemniscate γ_ρ we pick only a subset of test points, where we compare the exact value $H_n(z)$ to the approximate values with added errors. First we take $k = 10$ equally spaced points ϕ from the interval $[0, 1]$. To get points from the lemniscate we solve the roots of

$$p(z) = \rho \cdot e^{i2\pi \cdot \phi},$$

with Matlab's 'root' command. This returns $d = 3$ roots for each ϕ, i.e. we have 30 test points to examine for each n and ρ. To compare the effect of the size ρ to the maximum error at these 30 points we use levels in the Table 4.1. The corresponding lemniscates are drawn in Figures 1 and 2.

At each test point we calculate the exact value $H_n(z)$ (turned to a double precision floating point number) and the numerically computed (with added errors) of each

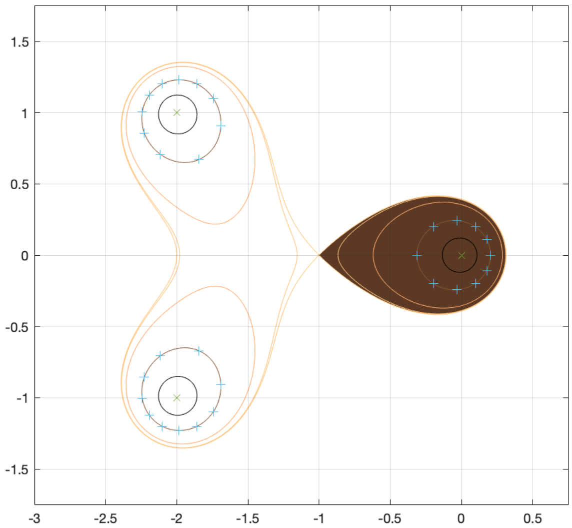

Figure 2: (Example 2) Level curves of polynomial $p(z) = z(z^2 + 4z + 5)$ with roots $\lambda_1 = 0$, $\lambda_2 = -2 + i$, and $\lambda_3 = -2 - i$. The roots are marked with 'x'. There are two critical points c, $p'(c) = 0$, $c_1 = -1$ and $c_2 = -5/3$. At corresponding level $|p(c_1)| = 2 =: \rho_{crit}$ the two remaining components join together. The component including the root $\lambda_1 = 0$ is colored. Four sets of smaller level curves γ_ρ where ρ is $t \times \rho_{crit}$ and t is either 0.30, 0.60, 0.90 or 0.99 are drawn in addition to the lemniscate $|p(z)| = \rho_{crit}$. Example of the testpoints used in our numerical calculations are marked with '+' on the lemniscate $|p(z)| = 0.6 \times \rho_{crit}$.

version of the (4.1)–(4.4).

4.2 Results

We test each of the variables ρ, ν, and μ separately for both Examples 1 and 2. In each case we compare the maximum error of each algorithm at the test points for each ρ. In all figures the amount of the derivative data n on the x-axis will have values $4 : 4 : 24$. The values between these would only add a little variation to graphs, but they would not change the behavior between algorithms. In the graphs y-axis is logarithmic and errors larger then 1 are not drawn.

4.2.1 Level curves γ_ρ

In Figure 3 the values ν and μ are both 0. We see the effect of rounding errors from double precision Horner's algorithm and the error from the location of the test points from different lemniscates γ_ρ. We use four different levels ρ in the numerical examples. The test points are taken from level curves where ρ is $t \times \rho_{crit}$ and t is either 0.30, 0.60, 0.90 or 0.99. The numerical values for both examples are listed in Table 4.1.

In all cases the error in Hermite polynomial $H_n(z)$ grows exponentially as expected. In the Parallel case $T_n(z)$ errors stay small only near the roots. Otherwise the growth in errors exceeds exponential growth and grow even faster as ρ grows. The Special version grows exponentially as well, but in a much slower fashion compared to Hermite and Parallel versions. The Multicentric version stays practically constant in all cases.

Even with small value of ρ we can see that the double precision arithmetic is the larger source of error in evaluations. The errors caused by ν and μ will not be visible with a large value of ρ. We will use $\rho = 0.02 \times \rho_{crit}$ in the following tests for the effect of ν and μ.

4.2.2 Evaluation error ν

We use $\mu = 0$ for rounding error, $\rho = 0.02 \times \rho_{crit}$ and $n = 4 : 4 : 24$. The results are in Figure 4.

In all cases Multicentric stays within reasonable error size i.e. from $1 \times \nu$ to $10 \times \nu$ on the logarithmic scale. Parallel and Special show similar behavior. The error stay almost constant as n grows. In Example 1 in the two largest values of μ the Special and Parallel algorithms outperform the Multicentric algorithm.

4.2.3 Rounding error μ

We use $\nu = 0$ for evaluation error, $\rho = 0.02 \times \rho_{crit}$ and $n = 4 : 4 : 24$. The results are in Figure 5.

In all cases Multicentric stays again within reasonable error size i.e. $(1 - 10) \times \nu$ on the logarithmic scale unlike the other algorithms. The error growth is modest for Special and Parallel but do exceed the limits $10 \times \nu$.

4.3 Conclusions

To calculate $\varphi(A)$ using traditional methods we need to know the eigenvalues exactly. The benefit of the Multicentric representation for φ is that we can use approximate values for the eigenvalues. To compensate the lack of knowledge we do need to calculate the expansion for larger n, but as we can see from Figure 6 for $n = 4 : 8 : 100$ the Multicentric version keeps the error at constant and approximately the same size as the added errors. This allows to use as much derivative data as needed. For Multicentric algorithm it is possible to compute the polynomials used numerically without additional errors, but not for the other algorithms, see Figure 7.

References

[1] Diana Andrei. Multicentric holomorphic calculus for n-tuples of commuting operators. *Adv. Oper. Theory*, 4(2):447–461, 2019.

[2] Diana Andrei, Olavi Nevanlinna, and Tiina Vesanen. Rational functions as new variables. *Banach J. Math. Anal.*, pages 16–37, 2022.

[3] Diana Apetrei and Olavi Nevanlinna. Multicentric calculus and the Riesz projection. *Journal of Numerical Analysis and Approximation Theory*, 44(2):127–145, 2016.

[4] M. Fekete. Über die Verallgemeinerung der Picard-Landauschen und Picard-Schottkyschen Sätze auf Reihen, die nach Potenzen eines Polynoms fortschreiten und Polynome niedrigeren Grades zu Koeffizienten haben. *Math. Ann.*, 106:595–616, 1932.

[5] C.G.J. Jacobi. Über Reihenentwicklungen, welche nach den Potenzen eines gegebenen Polynoms fortschreiten, und zu Coeffizienten Polynome eines niedereren Grades haben. *J. Reine Angew. Math.*, 53:103–126, 1856-1857.

[6] Aristides I. Kechriniotis, Konstantinos K. Delibasis, Christos Tsonos, and Nicholas Petropoulos. A new parallel polynomial division by a separable polynomial via Hermite interpolation with applications. *Electronic Journal of Linear Algebra*, 23:770–781, August 2012.

[7] A. Kienast. *Über die Darstellung der analytischen Funktionen durch Reihen, die nach Potenzen eines Polynomes fortschreiten und Polynome eines niedereren Grades zu Koeffizienten haben*. PhD thesis, Zürich, 1906.

[8] A. I. Markushevich. *Theory of Functions of a Complex Variable*, volume 2. Chelsea Publ. Co, second edition, 1977.

[9] O. Nevanlinna. Lemniscates and K-spectral sets. *J. Funct. Anal.*, 262:1728–1741, 2012.

[10] O. Nevanlinna. Multicentric holomorphic calculus. *Computational Methods and Function Theory*, 12(1):45–65, June 2012.

[11] O. Nevanlinna. Polynomial as a new variable - a Banach algebra with functional calculus. *Oper. and Matrices*, 10(3):567–592, 2016.

[12] T. Vesanen. Numerical computation of multicentric coefficients for monomials. *tba*, 2025.

[13] J. L. Walsh. *Interpolation and Approximation by Rational Functions in the Complex Domain*, volume 20 of *Colloquium Publications*. Amer. Math. Soc., fifth edition, 1969.

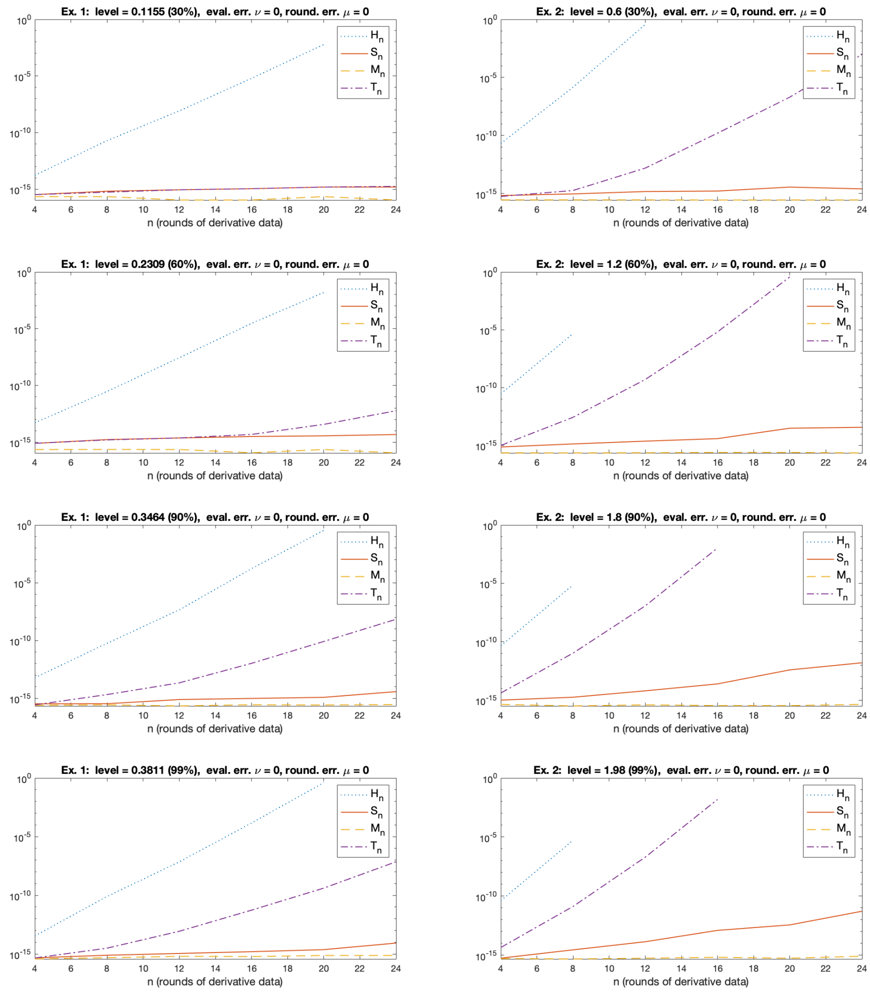

Figure 3: (Example 1 in the left column and Example2 on the right hand side) Effect of the size of ρ. The errors ν and μ are zero. The smallest level $\rho = 0.3 \times \rho_{crit}$ is in the first row and the levels grow with each line according the Table 4.1.

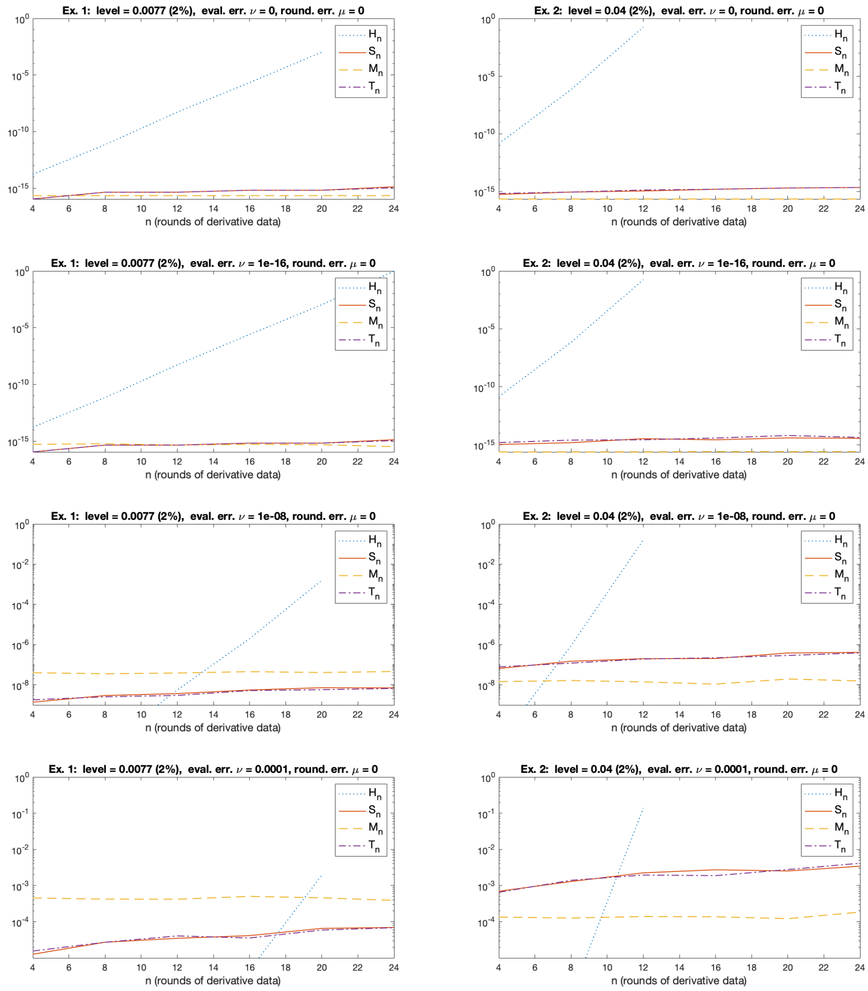

Figure 4: (Example 1 on the left and and 2 in the right hand side column) Effect of evaluation error ν when $\rho = 0.02 \times \rho_{crit}$ and rounding error $\mu = 0$. The tested values for ν are 0, 10^{-16}, 10^{-8}, and 10^{-4} (from top to bottom).

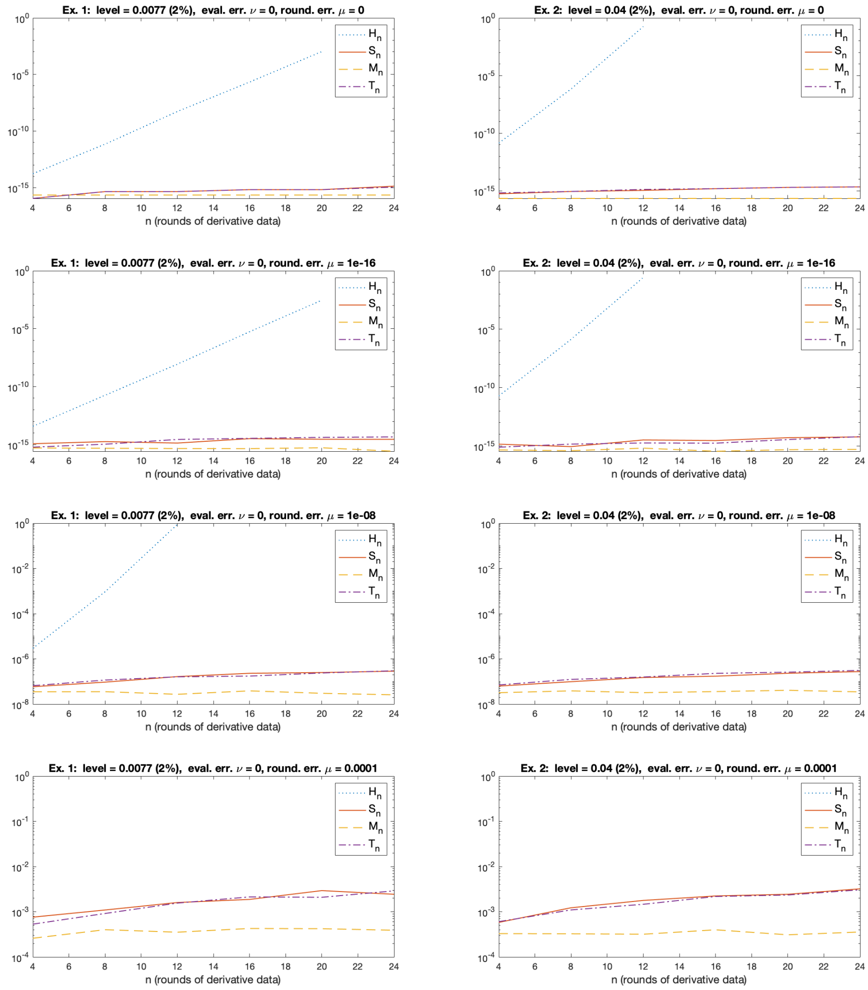

Figure 5: (Example 1 on the left and 2 on the right) The effect of rounding error μ when $\nu = 0$ and $\rho = 0.02 \times \rho_{crit}$. Values used for μ are 0, 10^{-16}, 10^{-8}, and 10^{-4} (from top to bottom). The error values for Special (red contiguous line) on the bottom right are $6.54 \cdot 10^{-4}$ at $n = 4$ and $2.9 \cdot 10^{-3}$ at $n = 24$.

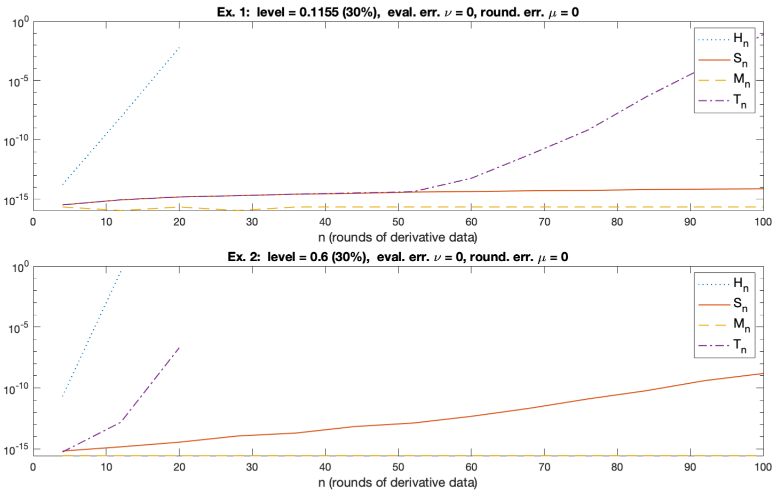

Figure 6: (Example 1 (top) and 2 (bottom)) The effect of large values for the number of round of derivative data n, where $n = 4 : 8 : 100$. Other variables are kept fairly small, $\rho = 0.30 \times \rho_{crit}$, or zero as $\nu = \mu = 0$.

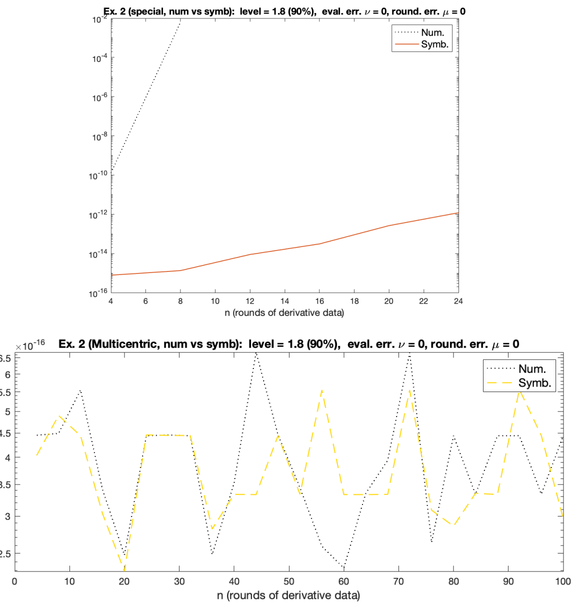

Figure 7: From the top graph we see that computing the coefficients numerically introduces drastically more errors for the Special algorith in the Example 2 with $\rho = 1.80$ (90%). (For Parallel algorithm the results were even worse than this.) With Multicentric the difference between symbolically and numerically computed coefficients stays withing 10^{-16} even for large values n in the bottom graph.